23rd International Symposium on Transport Phenomena
Auckland, New Zealand
19–22 November 2012

Condensation Control in Glazed Flat Plate Solar Water Heaters

J. Oshikiri[1] and T.N. Anderson[1]

[1]School of Engineering
Auckland University of Technology, Auckland 1142, New Zealand

Abstract

Glazed flat plate solar collectors offer a simple and cost effective approach to heating water. However, on clear nights solar collectors can transfer a significant amount of heat to the atmosphere by radiation. In areas with a cool climate and high relative humidity the radiation heat loss can lead to the temperature of the glazing often reaching the dew-point of the surrounding air, this leads to condensation developing on the glazing. If water condenses on the inside of the glazing and repeatedly drips onto the solar absorber this could lead to damage of the solar collector surface thus shortening its operating life. Also the build-up of condensation on the glazing can lead to the growth of mould, is visually displeasing to the owner, and means energy must be "wasted" to evaporate the moisture during the following day.

This study aims to develop the understanding of the role that condensation plays on collector performance, as well as addressing ways of minimising the impact it has. In doing so it presents an experimentally validated, numerical model for determining the frequency of condensation in glazed flat plate solar water heaters. It shows that climatic factors including relative humidity, ambient temperature and wind speed determine the frequency of condensation for any given location. However, it also reveals that the frequency of condensation can be modified by altering the convection heat transfer coefficient inside the collector and most significantly by using low emissivity coatings on the glazing layer.

Introduction

Modern society relies deeply on the use of fossil fuels, and it is generally understood that they cause some negative impacts on the environment. Solar energy is a promising alternative to this, as it can substitute fossil fuels in a clean and renewable manner. The use of solar water heating is widespread, particularly in Germany, China and Australia due to the fact that it can be cost effective and last for over 20 years.

However, over time the performance of solar water heaters decreases due to the corrosion and degradation of the materials inside the collector. A study conducted under the auspices of the International Energy Agency's Solar Heating and Cooling Program suggested that the main reason for corrosion could be due to condensation inside the collector [1].

Condensation is a natural phenomenon often associated with enclosed spaces such as refrigerators, buildings and vehicles, due to changes in temperature and humidity. However, solar thermal flat plate collectors can also suffer from condensation problems, particularly in cold areas with high relative humidity such as continental and northern Europe [1] and southern areas of Australia.

The mechanism of condensation in a solar thermal flat plate is principally driven by the release of heat into the atmosphere by radiation, particularly at night. If the temperature in the collector cover falls below the dew point temperature, condensation can form on the glazing of the collector. The existence of water can cause damage to the collector surface and create unfavourable microclimatic conditions for the internal materials. In addition to this, energy must be used to evaporate the moisture the next day.

Even in a small flat plate solar thermal collector, a great deal of moisture condensation can occur, and repeated condensation dripping onto the solar absorber can lead to a degrading of the collector over time. Despite previous studies focussing on European climates, corrosion due to condensation and its impacts on the performance of solar water heating systems is also a significant problem in New Zealand [2-4].

In light of problems posed by condensation in flat plate solar water heaters and the relative lack of attention paid to the problem, this study set out to explore ways of reducing the occurrence of condensation in flat plate solar collectors, particularly in New Zealand.

Theoretical Modelling

Heat Balance

In order to analyse the frequency of condensation in a flat plate solar water heater it was decide to utilise a quasi-steady state numerical model to determine the temperature and relative humidity inside the collector.

In this model, it was assumed that the heat transfer in the collector was one-dimensional and as such the temperature of the collector surfaces were uniform, such that there was no difference in temperature between the corners and the centre of the collector.

Figure 1 illustrates a cross sectional view of a typical single glazed collector, showing the heat transfer mechanisms, where T_a is the ambient temperature and T_i is the temperature inside the collector.

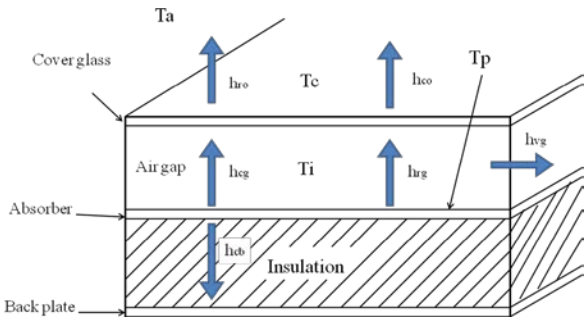

Figure 1. Cross sectional view of a collector

To determine the absorber and cover temperature, it is essential to calculate the heat transfer by convection, conduction and thermal radiation from all the surfaces and in the solar collector. This can be done by iteratively solving the collector heat balance equations (Equation (1) and (2)) for a collector of unit area [1].

$$C_p \frac{dT_p}{dt} = G(\tau\alpha) - h_{cb}(T_p - T_a) - h_{cg}(T_p - T_c) - h_{rg}(T_p - T_c) \quad (1)$$

$$C_c \frac{dT_c}{dt} = Ga_c + h_{cg}(T_p - T_c) + h_{rg}(T_p - T_c) - h_{vg}(\frac{T_p + T_c}{2} - T_a) \quad (2)$$
$$- h_{co}(T_c - T_a) - h_{ro}(T_c - T_s) - q_{ei} - q_{eo}$$

In equations (1), (2), G is the incident solar radiation and $\tau\alpha$ is the transmittance-absorptance product of the solar collector, h_{cb} is the heat loss through the back insulation, h_{cg} and h_{rg} represent the heat transfer coefficient for natural convection and thermal radiation in the air gap respectively. h_{ro} is the heat transfer coefficient for thermal radiation from the cover to the ambient air and h_{co} is the heat transfer by convection from the cover to the ambient air. The heat transfer coefficient due to ventilation was expressed by h_{vg}. Finally, q_{ei} and q_{eo} are the heat transfer by evaporation and condensation.

The conductive heat loss through the back insulation material h_{cb} was given by a modified form of Fourier's law (Equation (3)) where e_i is the thickness of the insulation and k_i the thermal conductivity.

$$h_{cb} = \frac{k_i}{e_i} \quad (3)$$

The convective heat transfer coefficient between the absorber and the glazing (h_{cg}) (Equation 4) [1] is expressed in terms of three parameters: the thermal conductivity of air (k_0), the thickness of the air gap (e_o) and the Nusselt number (Nu_g). The Nusselt number is a function of the slope of the collector, which has a significant influence on the performance of the collectors across the year.

$$h_{cg} = \frac{Nu_g k_0}{e_g} \quad (4)$$

The Nusselt number can be determined by a correlation between the Nusselt number and Rayleigh number for tilt angles from 0 to 75°as expressed by equation (5) [5]:

$$Nu_g = 1 + 1.44\left[1 - \frac{1708}{Ra_g \cos s}\right]^+ \left(1 - \frac{(\sin 1.8 \cdot s)^{1.6} \cdot 1708}{Ra_g \cos s}\right) \quad (5)$$
$$+ \left[\left(\frac{Ra_g \cos s}{5830}\right)^{0.33} - 1\right]^+$$

In equation (5), the positive symbol indicates that if the values in the square brackets are negative, the values will be zero. Rayleigh number for air inside the collector (Ra_g) is give by equation (6).

$$Ra_g = \Pr \cdot \frac{g\beta(T_p - T_c)e_g^3}{\nu^2} \quad (6)$$

where β is the volumetric coefficient of expansion of the air given by equation 7.

$$\beta = \frac{2}{T_P + T_c} \quad (7)$$

The heat transfer due to radiation from the cover to the sky and to the surrounding ground (h_{ro}) is given by Equation 8 [1].

$$h_{ro} = 0.5(1 + \cos s)\varepsilon_c C_s \left(\frac{T_c^4 - T_s^4}{T_c - T_s}\right) \quad (8)$$
$$+ 0.5(1 - \cos s)\varepsilon_c C_s \left(\frac{T_c^4 - T_a^4}{T_c - T_s}\right)$$

Where the view factor to each is taken to be 0.5 and T_s is the sky temperature. The sky temperature can be expressed using the dew point temperature and the time from midnight as shown in Equation 9 [5].

$$T_s = T_a\left[0.711 + 0.0056T_{dp} + 0.000073T_{dp}^2 + 0.13\cos(15t)\right]^{\frac{1}{4}} \quad (9)$$

Where T_{dp} is the dew point temperature and t is the number of hours from midnight. Equation (9) is effective for a dew point temperature from -20℃ to 30℃ and clear sky conditions, however, for this study it was assumed to be valid for all conditions.

The heat transfer by convection from the cover to the ambient air (h_{co}) can be expressed in terms of the collectors' characteristic length (L), the Nusselt number due to convection (Nu_0) and the thermal conductivity of air (k_g) as illustrated by equation (10).

$$h_{co} = Nu_0 \frac{k_g}{L} \quad (10)$$

The Nusselt number for convection (Nu_0) is calculated from the square root of the Nusselt number for laminar flow and turbulent flow as shown in equation (11). The Nusselt number is given by the product of Reynolds number and Prandtl number for laminar and turbulent flow as shown in equation (12) and (13) [1].

$$Nu_0 = \sqrt{Nu_{lam}^2 + Nu_{turb}^2} \quad (11)$$

$$Nu_{lam} = 0.664\,\mathrm{Re}_+^{0.5}\,\Pr^{0.33} \quad (12)$$

$$Nu_{turb} = \frac{0.037\,\mathrm{Re}_+^{0.81}\,\Pr^{0.33}}{\left(1 + 2.443\,\mathrm{Re}_+^{-0.1}(\Pr^{0.67} - 1)\right)} \quad (13)$$

The Reynolds number (Re) is a dimensionless number representing the ratio of inertial forces to viscous forces. In equation (14) the overall Reynolds number Re_+ is taken to be the sum of a forced and free component [5].

$$\mathrm{Re}_+ = \sqrt{\mathrm{Re}^2 + \mathrm{Re}'^2} \quad (14)$$

The Reynolds number for forced flow Re on the cover of the collector can be determined from three elements: wind speed (V_w), kinematic viscosity (ν) and characteristic length (L) as shown in equation (15) [1].

$$\mathrm{Re} = V_w \frac{L}{\nu} \quad (15)$$

The Reynolds number (Re') for natural convection is calculated by defining an equivalent Reynolds number and is given by equation (16) [6].

$$\mathrm{Re}' = 0.64Gr^{0.5} \quad (16)$$

In equation (16) the Grashof number (Gr) is a non-dimensional parameter used to quantify the heat transfer due to natural convection and between the cover and the ambient air and is given by equation (17) [1].

$$Gr = 2 \cdot L^3 \cdot g \frac{(T_c - T_a)}{v^2 (T_a + T_c)} \quad (17)$$

Now it assumed that condensation occurs if the cover temperature falls the dew point temperature. Under these conditions the heat transfer by condensation and evaporation of moisture at the outer cover is expressed by equation (18) and (19). Now Equation (18) and (19) were developed for condensation, however, it was assumed that it is valid for evaporation even though evaporation takes place only the cover is wet [1].

$$T_c \geq 0 : q_{eo} = 0.017 \cdot h_{co} \{p_{ws}(T_c) - p(T_{dewa})\} \quad (18)$$

$$T_c \leq 0 : q_{eo} = 0.019 \cdot h_{co} \{p_{ws}(T_c) - p(T_{dewa})\} \quad (19)$$

The evaporation heat loss from the inside of the cover (q_{ei}) is expressed by the mass transfer rate of air through the air gap and the latent heat of water. Equation (20) shows heat transfer by evaporation or condensation at the inside of the cover [5].

$$q_{ei} = m_{vg} h_{fg} \quad (20)$$

The heat transfer coefficient because of ventilation (h_{vg}) is obtained from equation (21) [1].

$$h_{vg} = m_{vg} C_{pa} \quad (21)$$

Finally, the thermal radiation heat transfer coefficient between the absorber and the cover (h_{rg}) can be expressed by Equation 22 [5].

$$h_{rg} = \frac{C_s (T_p^4 - T_c^4)}{(\frac{1}{\varepsilon_p} + \frac{1}{\varepsilon_c} - 1)(T_p - T_c)} \quad (22)$$

Ventilation Effects

In Equation 20 and 21 reference was made to the ventilation rate of a solar collector; typically ventilation is caused by two main factors: thermal driven pressure due to heating and cooling of the solar collector (through cracks or manufacturer's ventilation ports) as well as wind driven pumping effects. Ventilation which includes all elements is overly complex to model, so only thermal driven pressure was considered in this model.

The driving pressure is the pressure difference caused by the pressure loss of the distance. The driving pressure is given by the density of the air, the gravity and vertical co-ordinate measured from the neutral plane. When the humidity of air is considered, the differential pressure is give by equation (23) [1].

$$\Delta P = \left(\rho(T_a, P_{wa}) - \rho\left(\frac{T_p + T_c}{2}, P_{wg} \right) \right) h \cdot g \quad (23)$$

Where, P_{wa} is partial pressure of water in the open air and P_{wg} is partial pressure of water in the air of the air gap in the collector.

Moist air density (ρ_a) is defined as the reciprocal of the moist air specific volume (V). The density of the moist air density is calculated as shown in equation (24) [1].

$$\rho_a = \frac{1}{V} \quad (24)$$

The specific volume of the moist air is expressed as equation (25) and the humidity ratio of moist air (W) is defined by equation (26) [1].

$$V = \frac{R_a T}{p}(1 + 1.6078W) \quad (25)$$

$$W = 0.62198 \frac{p_w}{p - p_w} \quad (26)$$

The mass flow of damp air is given equation (32) [1].

$$m_{vg} = 0.5 \left(\rho(T_a, P_{wa}) + \rho\left(\frac{T_a + T_c}{2}, P_{wg} \right) \right) V \cdot \Delta P \quad (27)$$

For the simulation the mean value is used for the density of the air.

Moisture Balance

From the previous sections, the temperature inside the collector was obtained. It was assumed that the volume of the collector was constant, and then Charles's law and Boyle's law are used to calculate the pressure in the collector (Equation (28)). Where P_a is the atmospheric pressure in open air and P_c is the pressure inside the collector.

$$\frac{P_a}{T_a} = \frac{P_c}{T_i} \quad (28)$$

In conducting the moisture balance we need to consider the partial pressure of water (Equation (29)) where P_{ca} is partial pressure of dry air inside the collector and P_{cw} partial pressure of water vapour inside the collector.

$$P_c = P_{ca} + P_{cw} \quad (29)$$

The humidity ratio of moist air (w) is defined as the ratio of the mass of the water vapour (m_w) to the mass of the dry air (m_{da}) as shown in equation (30).

$$w = \frac{m_w}{m_{da}} \quad (30)$$

As such the moisture inside the collector is given by equation (31).

$$W_i = 0.62198 \frac{P_{cw}}{P_c - P_{cw}} \quad (31)$$

Any moisture in the insulation was ignored and, the saturated vapour pressure inside of the collector (P_{cw}) was assumed to be equal as the saturated vapour pressure outside. The saturated vapour pressure outside was calculated from relative humidity outside.

Experimental Method

To validate the numerical model, an experiment to measure the absorber temperature, cover temperature and relative humidity in the air gap was developed. A single glazed flat plate solar collector 1 meter long and 1.8 meters wide and was positioned to face due north at an angle of 37° to the horizontal (Figure 2).

The collector was fitted with nine T-type thermocouples (±0.3°C), four of which were attached to the surface of absorber, another four were attached to the inside surface of the cover and the last thermocouple was used to measure the ambient temperature. The sensors for absorber and cover were uniformly distributed over the surfaces to determine the mean surface temperatures.

In addition, two relative humidity sensors (Honeywell, HIH-4000) were used to measure relative humidity inside the collector air gap and in the ambient air. A pyranometer (Apogee, SP110)

was used to measure the global radiation incident the collector. Additionally atmospheric pressure and local wind speed was recorded by the AUT weather station. The data from the experiment was recorded at ten minute intervals and saved in a spreadsheet, to allow comparison with the simulated data.

Figure 2. Experimental solar collector

Experimental Results and Model Validation

Though the experimental data was collected over a relatively long time-frame for clarity, and brevities sake, experimental data is presented for just one test day. Figure 3 shows the observed incident radiation, ambient temperature and wind speed for a typical test.

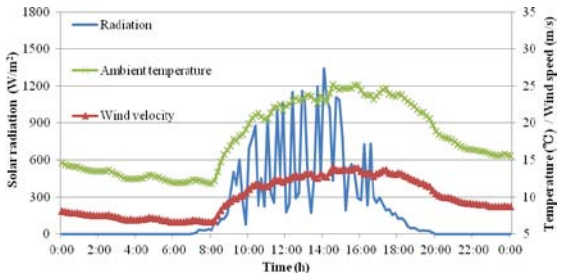

Figure 3. Meteorological conditions for a typical test

To examine the validity of the model, the results of an experiment and a simulation using the measured meteorological inputs (temperatures, barometric pressure, solar radiation and wind speed) and the design characteristics of the collector model were compared.

In Figure 4, the measured absorber temperature is compared with the simulated absorber temperature. The absorber temperature fluctuations are the result of the variation in the incident radiation and also the time interval over which the measurements were recorded, and the simulation discretised. However, it can be seen that, in general, the simulation was able to predict the absorber temperature relatively well, especially at night when condensation might occur.

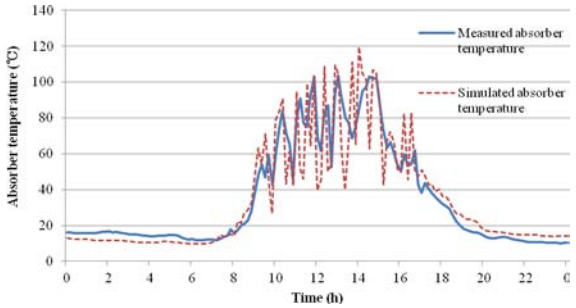

Figure 4. Measured v predicted absorber temperature

Similarly, in Figure 5, the measured and simulated cover temperature are compared, the simulated cover temperature showed almost the same temperature as the measured cover temperature. The difference in temperature during the day is predominantly due to the thermocouple junctions absorbing radiation. However, it can be seen that the simulation was able to predict the cover temperature quite well at night when condensation might occur.

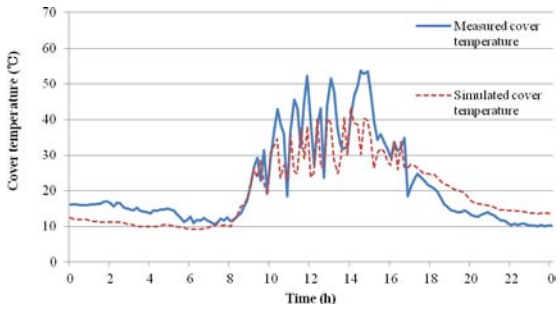

Figure 5. Measured v predicted absorber temperature

Having been able to provide a relatively accurate prediction on the collector temperatures the measured and simulated relative humidity' in the air gap of the collector were compared. In Figure 6 it can be seen that there is a minor difference between simulated and measured relative humidity.

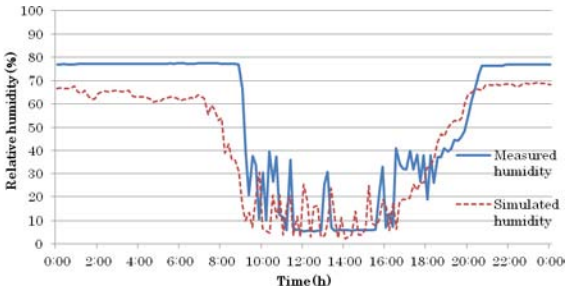

Figure 6. Measured v predicted absorber temperature

On the whole, the simulated relative humidity shows the same trend as the measured data, in that it dropped around 9am as the sun went up and increased after 6pm as the sun went down. In Figure 6, it can be seen that in the morning and at night, there is a small difference between measured humidity and simulated humidity. There are a number of reasons why this may occur, in particular, the effect that uncontrolled ventilation due to wind has on the collector and also the assumption that the water vapour pressure in the collector was assumed to be same as in open air.

Despite these differences though, the simulation can predict a change of relative humidity inside of the collector fairly

accurately and as such should be able to provide an insight into the occurrence of condensation.

As a final test of the model a verification test was carried out to test the model's ability to predict the occurrence of condensation. After the experimental testing of temperatures and humidity's had been completed, the collector experienced an evening of very clear skies and high humidity such that moisture was found on the collector at 8am on March 22 as shown in Figure 7.

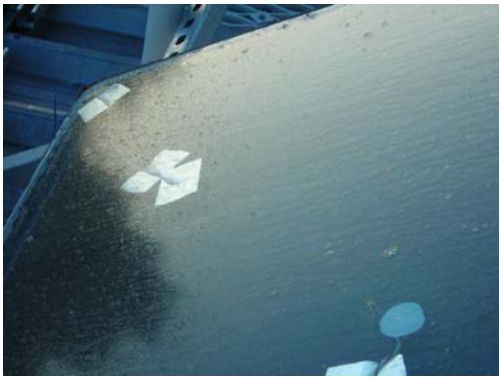

Figure 7. Condensation on collector

Therefore a simulation was conducted retrospectively using meteorological data collected from the National Institute of Water and Atmosphere's (NIWA) Cliflo database [7]. Figure 8 shows the simulated absorber, cover temperature and the dew point temperature from NIWA Cliflo database.

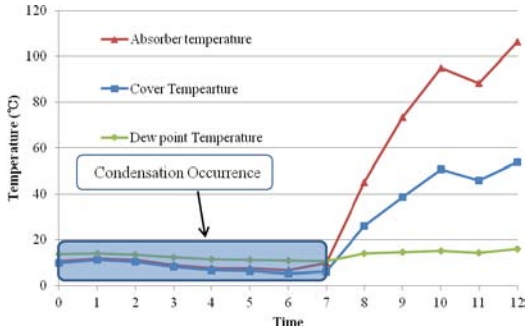

Figure 8. Modelled results of observed condensation occurrence

From the simulation, if it is assumed that condensation occurs on the surface of the collector when the cover temperature is lower than the dewpoint temperature, condensation could occur until 7:30am. However, because the weather information from the NIWA Cliflo database was collected and applied to the simulation, the location was not exactly the same as the test site. Therefore, the condensation persisted slightly longer than the model would predict. However, the model helped to predict the occurrence of condensation on the collector and provided a relatively accurate prediction of its duration.

Sensitivity Analysis

Having demonstrated the models ability to predict condensation it was decided to undertake a modelling sensitivity analysis of a copper single glazed collector to better understand the factors that influence the frequency of condensation in New Zealand solar collectors. To do this it was decided to vary the location, collector slope, ventilation rate and the emissivity of the cover, taking July 1st as the test day.

Influence of location on condensation frequency

To determine the effect of location on the occurrence of condensation the model was tested for Auckland, Hamilton, Wellington, and Christchurch in New Zealand for the year 2010 using weather data from the NIWA Cliflo database. In Figure 9, the simulated relative amount of condensation time in each month for 2010 for each city is shown. It can be seen that in the winter season condensation occurs more than in the summer season in any location.

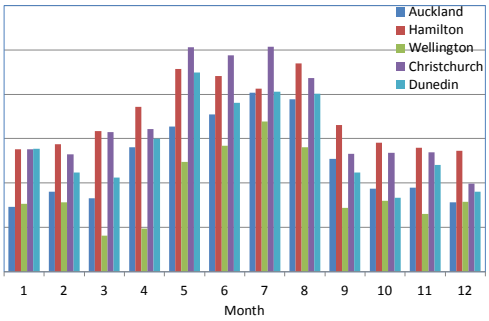

Figure 9. Modelled results of observed condensation occurrence

From Figure 9 it can be seen that in Auckland, the simulated total amount of condensation time in winter reached more than double that in the summer season. Hamilton shows a similar trend, though the predicted annual condensation hours were significantly higher than Auckland. This can be explained by the fact that, according to NIWA, in 2010, the average wind speed in Hamilton was 2.8 m/s, which is quite low, and the relative humidity was 80 %, which is relatively high. As a result, the frequency of condensation hours in Hamilton was significantly higher than the other places, thus illustrating that climatic factors including relative humidity and wind speed play a significant role in the occurrence of condensation on a surface of the collector.

Similarly the annual simulated condensation hours in Wellington were considerably lower than Auckland. Wellington is famous for its southerly blasts in winter and the city is generally very windy all year. The average wind speed in Wellington was approximately 6.9 m/s which was significantly faster than the wind speed in Auckland. As a result, the frequency of condensation hours in Wellington was significantly lower than the other places.

Furthermore, the simulation was also run by using the data in Christchurch, it can be seen that the frequency of simulated condensation hours in winter is higher than the other cities. In Christchurch in winter, relative humidity is considerably high and the ambient temperature can drop below 0 °C at night, so ground frost is common in winter. As such it can be deduced that the ambient temperature can be one of the climatic factors which influence the frequency of condensation.

In summary, the results illustrate that the frequency of condensation on the surface of the cover was considerably influenced by three climatic factors: ambient temperature, wind velocity and relative humidity. It was found that areas with a low mean wind velocity and high relative humidity, such as Hamilton, and with cold weather, such as Christchurch, had a high frequency of condensation.

Influence of the slope of the collector on condensation frequency

Now when considering changing the location of a collector, one would change the slope of the collector to maximise the solar radiation collected. In the modelling, changing the slope of the collector influences two heat transfer parameters h_{cg} and h_{ro}. h_{cg} represents the heat transfer coefficient for natural convection in

the air gap, and h_{ro} is the heat transfer coefficient for thermal radiation from the cover to ambient air. Figure 10 shows the relationship between the slope of the collector and h_{cg} and h_{ro} at night. At night, h_{cg} was not influenced by any collector slope. On the other hand, h_{ro} was decreased as increasing of slope of the collector. Figure 10 shows that increasing of the slope of the collector decreases the thermal radiation from the cover to the ambient at night, as the collector sees the warm ground.

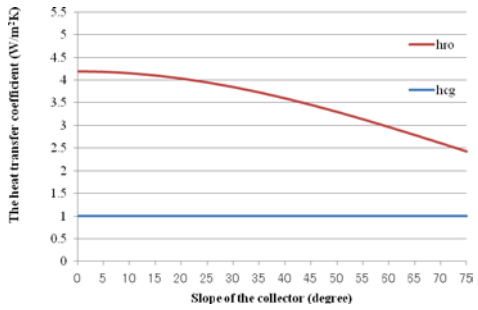

Figure 10. The relationship between the slope of the collector and h_{cg} and h_{ro} during the night

In exploring this further the slope of the collector was also changed, the slope was set as 15°, 30°, 45°and 60°. Figure 11 shows the relationship between the number of expected condensation hours and slope of the collector. This indicates that increasing of the slope of the collector has an impact on condensation on the surface of the collector, though it is relatively minor.

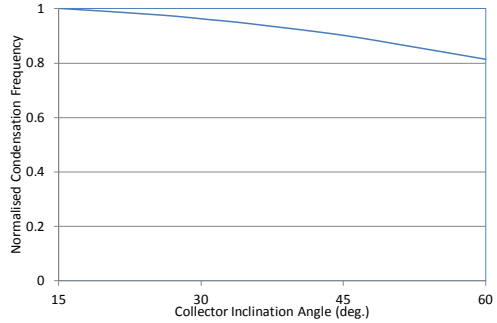

Figure 11. Effect of slope of the collector on condensation hours

Influence of ventilation of the air gap on condensation frequency

Now in the development of the model, accounting for heat transfer due to ventilation is perhaps the most complicated parameter to physically realise. This is because it is heavily dependent not only on the design of the collector, but also the quality of its construction. Therefore, during the simulation, the convection heat transfer coefficient was varied as a proxy for the ventilation rate of the collector.

As such h_{vg} was changed from 0 to 40 W/m^{2}K. Figures 12 and 13 show the effect of varying h_{vg} to 0.1, 10 and 40 W/m^{2}K has on the simulated absorber and cover temperatures. In this regard a high h_{vg} implies high ventilation of the air gap in the collector. Figures 12 and 13 show the same trend, that increasing ventilation eliminates the distinction between the temperature inside and outside the collector at night and during the day as it decreases the surface temperature of absorber and cover.

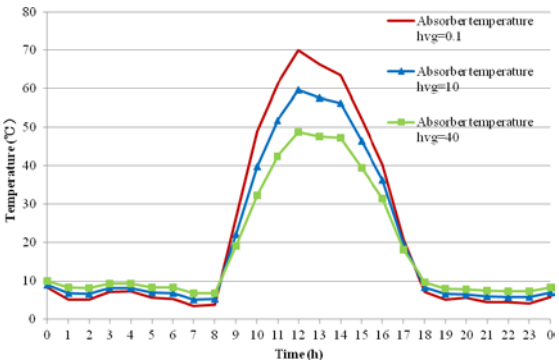

Figure 12. Absorber temperature with changing ventilation

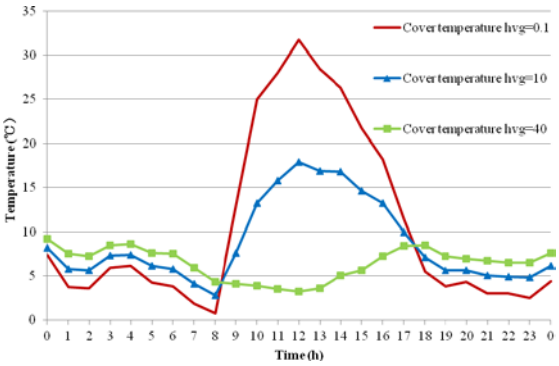

Figure 13. Cover temperature with changing ventilation

Figure 14 shows the relationship between ventilation rate and the number of expected condensation on the surface of the collector cover. It is shown that ventilation can be effective in reducing condensation however high ventilation is not always effective when compared to stagnant conditions.

This can be because of two important things to consider in controlling the surface condensation [8]: gaining low vapour pressure by ventilation and reduced moisture input and gaining high surface temperatures by providing insulation or heat input.

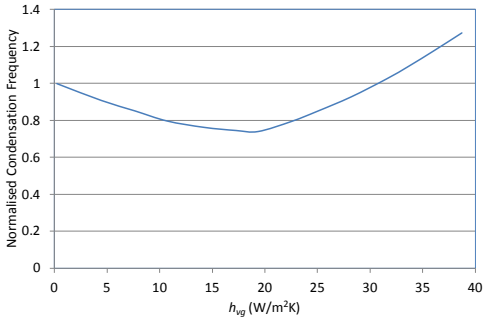

Figure 14. Effect of ventilation on condensation hours

Influence of cover emissivity on condensation frequency

As a final means of controlling the frequency of condensation, it was decided to explore the influence of the glass cover's emissivity on the phenomenon. Figure 15 shows the simulated absorber and cover temperature when the emissivity of the glass cover was 0.1 and 0.9. From this figure, it can be seen that the lower cover emissivity made the absorber temperature higher particularly during the day. On the other hand, changing the emissivity of the glass did not influence the cover temperature significantly.

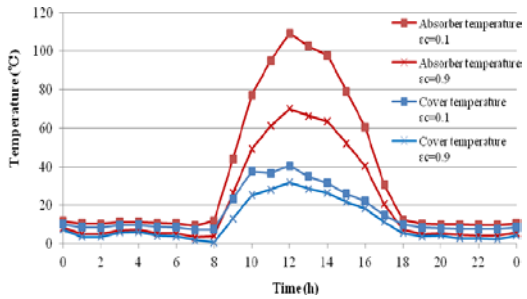

Figure 15. Effect of cover emissivity on absorber and cover temperature

Exploring this further, in Figure 16, the cover temperature declines as linear function, in contrast, the absorber temperature was decreasing as a quadratic function since radiation heat transfer is a function of T^4.

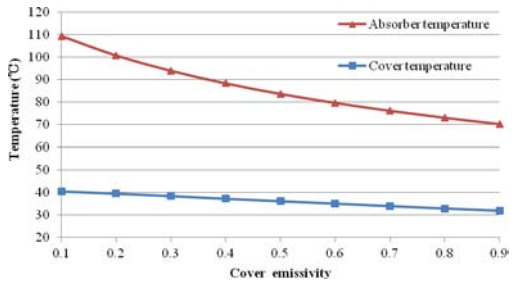

Figure 16. Relationship between the cover emissivity and the simulated absorber and cover temperatures

The implication of this is that a low emissivity coating on the glazing will lead to an improvement in the collector's efficiency. Furthermore Figure 17 shows the relationship of cover emissivity and the expected number of condensation hours in Auckland. The figure shows that cover emissivity significantly influences the frequency of condensation. As such, the use of low emissivity glass could be highly effective in preventing condensation. The simulation shows that using glass with an emissivity below 0.1 would effectively prevent condensation on the surface of the glass of the collector throughout the year in Auckland.

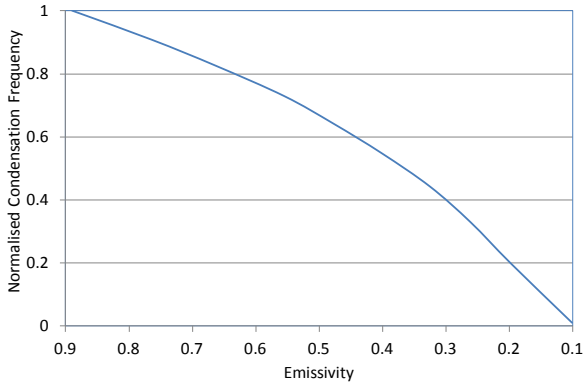

Figure 17. Effect of cover emissivity on condensation hours

Conclusions

Avoiding condensation in solar collectors is a critical issue in terms of their durability and performance. During the night the temperature of the collector will often drop below the ambient temperature due to thermal radiation in the cold air. In climates where the air at night becomes saturated with humidity, condensation will form both on the inside and outside of the collector glazing. If too much condensation occurs on the inside of the glazing, it will drip on to the absorber surface, which will consequently lead to long-term damage.

This study charted the development of a validated numerical model for examining condensation in flat plate solar water heaters. The numerical model showed that climatic factors including relative humidity, ambient temperature and wind speed can determine the frequency of condensation for any given location. Furthermore it also revealed that the frequency of condensation can be modified by altering the ventilation inside the collector, the slope of the collector and most significantly by using low emissivity coating on the glazing layer.

References

[1] Kohl, M., Carlsson, B., Jorgensen, G. and Czanderna, A. (editors), *Performance and durability assessment: Optical materials for solar thermal systems*, Oxford, Elsevier Ltd, 2004

[2] Kane, C.D. Pollard, A.R. and Zhao, J., *An Inspection of Solar Water Heater Installations, BRANZ Study Report No. 184*, Porirua, BRANZ, 2007

[3] Moller, G., *Solar water heating – Corrosion and performance issues in New Zealand*, 2007, http://rustypanelsblog.blogspot.co.nz/ [cited 1/05/2012]

[4] Television NZ, *Close Up [Television broadcast]*, Auckland, TVNZ, 2007, June 22

[5] Duffie, J and Beckman, W., *Solar engineering of thermal processes*, New Jersey, John Wiley & Sons, 2006

[6] Kreith, F. and Kreider, J., *Numerical prediction of the performance of high altitude balloons*, Boulder, National Center for Atmospheric Research, 1973

[7] The National Institute of Water and Atmospheric Research, *Cliflo database*, http://cliflo.niwa.co.nz/ [cited 2/03/2012]